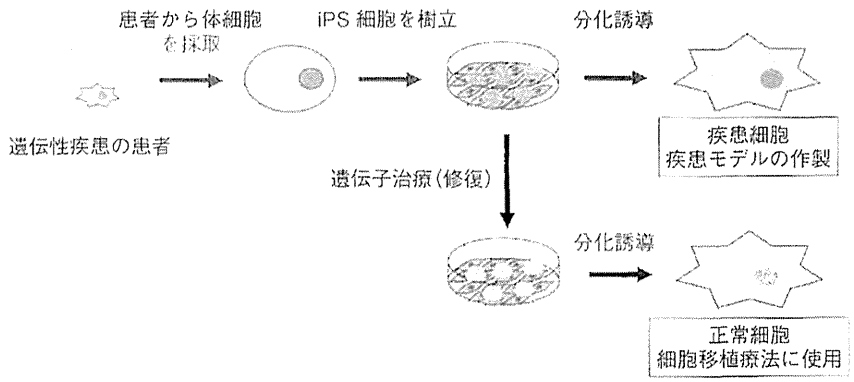


図8　遺伝性疾患における iPS 細胞技術を用いた疾患モデル作製と遺伝子治療
遺伝性疾患の患者体細胞から iPS 細胞を樹立し罹患細胞種に分化誘導すると，遺伝子変異が保持されているため疾患細胞が作製される。それらの細胞を用いて疾患モデルを構築できる。一方，樹立した iPS 細胞に遺伝子治療(修復)を行うことで，正常細胞を分化誘導可能となり，細胞移植療法に使用することができる

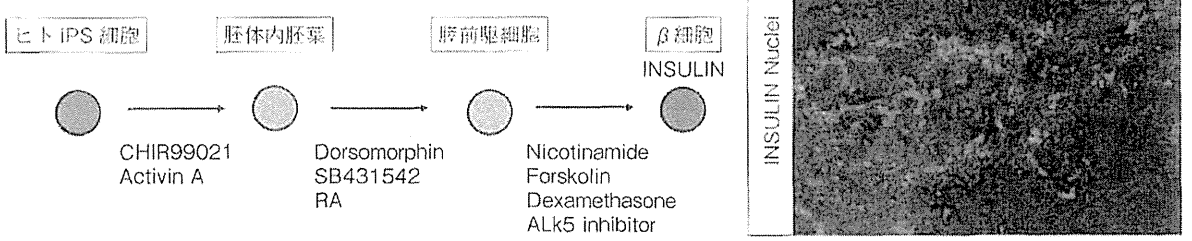


a：発生過程を模倣し，各段階で適切なサイトカインや化合物を加えて分化誘導を行う。ここでは当研究室の1例〔文献37)の分化誘導法を一部改変〕をあげる

b：ヒト iPS 細胞から分化誘導された膵細胞の抗インスリン免疫染色像

図9　iPS 細胞から膵β細胞への分化誘導

きなくても高率に血糖値の安定化が得られる。しかし，いずれの治療法にも依然としてドナー不足の問題が存在している。その解決策の1つとして，海外では無菌ブタの膵島を用いたバイオ人工膵島の移植がすでに臨床試験として行われているが，未知の感染症や異種拒絶のリスクがある。そのため，iPS 細胞から作製された膵細胞や膵組織を用いた移植療法の開発が期待されている。

1)　膵β細胞への分化誘導法の開発

膵島構成細胞のうちβ細胞が血糖値を検知してインスリンを分泌する働きを担う。よって，ES 細胞の樹立以降，種々のβ細胞への分化誘導法が検討されてきた。肝細胞と同様に生体内での発生過程を模倣し，iPS 細胞→胚体内胚葉→膵前駆細胞→内分泌前駆細胞→β細胞の順に，それぞれの段階で適切なサイトカインや化合物を加えることで分化誘導を行う（図9)。すでに多数の報告があるが，ヒト ES/iPS 細胞を用いた場合の分化誘導効率は，もっとも高いものでも25%程度でしかない[27]。しかも，β細胞のもっとも重要な機能である，グルコース濃度の上昇に応じてインスリン分泌量を増やす「グルコース応答能」を獲得した細胞を培養皿上で分化誘導した報告はほとんどない[28]。その理由として，膵発生のうち，膵前駆細胞から内分泌前駆細胞，β細胞への後半の機構がほぼ未解明のままであることがあげられる。その一方で，ヒト ES 細胞から膵前駆細胞まで分化誘導したものを免疫不全マウスに移植すると，3カ月以上経過した後にグルコース応答能を獲得したインスリン産生細胞が出現する[29)~30)]。したがって，現時点ではヒト ES/iPS 細胞から膵前駆細胞までの分化誘導は，自然発生と近いものと考えられる。

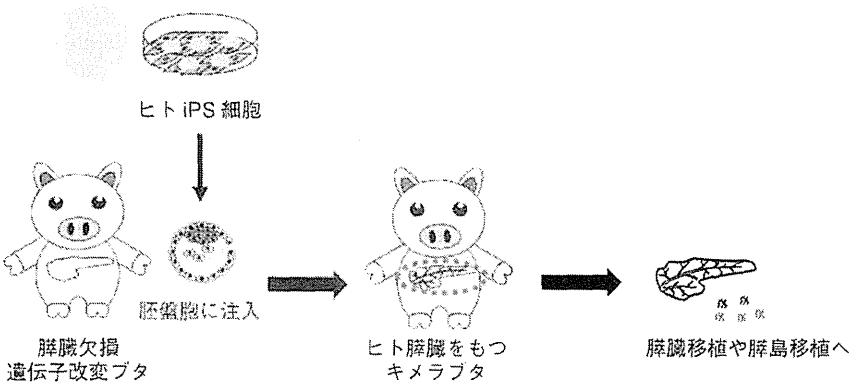


図10　胚盤胞補完法を用いたブタ体内でのヒト膵臓の作製
遺伝子改変によって膵臓を欠失するブタの受精卵胚盤胞にヒトiPS細胞を注入することで，ヒトiPS細胞由来の膵臓をもつキメラブタが作製できる可能性がある。実現すれば膵臓移植や膵島移植のドナー不足の解消に寄与することが期待される

2)　胚盤胞補完法

東京大学のNakauchiらのグループは，遺伝子操作により膵臓を欠失するマウスを作出し，そのマウスの受精卵胚盤胞にラットiPS細胞を注入する胚盤胞補完法と呼ばれる実験手法を用いて，マウスの体内にラットiPS細胞由来の完全な臓器としての膵臓を作製することに成功した[31]。さらに，Nakauchiらと明治大学のNagashimaらのグループは，遺伝子操作により膵臓を欠失するブタを作出し，胚盤胞補完法を用いて別の健常なブタの胚細胞を注入することで，完全なブタの膵臓を作製することにも成功した[32]。これらの成果から，胚盤胞補完法を用いることによって，膵臓をもたないブタの体内でヒトiPS細胞由来の膵臓を作製できる可能性が出てきた（図10）。実現すれば，作製されたヒト膵臓を用いる膵臓移植や膵島移植の開発が期待される。

3.　腸　管

短腸症候群，もしくは不可逆的な小腸機能不全（Hirschsprung病，先天性微絨毛萎縮症など）があり，さらに中心静脈栄養が継続困難な場合に小腸移植の実施が検討される。しかし，小腸はリンパ組織が豊富であるため，免疫反応が強いことが問題であり，とくに拒絶反応が強く出やすい。そのため，拒絶反応を回避し得る自己のiPS細胞を用いた腸管再生医療の実現が期待されている。米国シンシナティ小児病院医療センターのWellsらのグループは，腸幹細胞の三次元培養系[33]を応用することで，ヒトiPS細胞から機能的な腸上皮細胞や杯細胞，パネート細胞などを含む三次元の腸管様構造を作製することに成功した[34]。さらなる研究の進展が期待される。

## iPS細胞バンク

現時点において，iPS細胞を用いた自家移植を行うには，iPS細胞の樹立・安全性の確認・分化誘導などで移植実施までに数カ月から年余に及ぶ時間がかかると見込まれる。その期間を待機可能な疾患・症例であればよいが，急性期疾患などには対応できない。そのため，京都大学のYamanakaらは，2020年までに75種類のHLAホモ接合型のiPS細胞株を樹立・バンク化することを計画している。患者の少なくとも片方のHLA型が一致するiPS細胞株から分化誘導した細胞を移植に用いることで，拒絶反応の低減や移植後の長期予後の改善を図る。なお，統計学上，このHLAホモ接合型75種類で日本人の約80%をカバーできる。バンクにストックされたiPS細胞を用いることで自家移植ではなくなるが，iPS細胞樹立と細胞株の評価のステップを省くことで，移植細胞の準備にかかる時間が大幅に短縮されることが期待される。

## おわりに

近年の再生医学研究の急速な発展により，そう遠くない将来，消化器外科領域でもiPS細胞を用いた再生医療の実現が期待される。本稿が読者の皆様のiPS細

胞研究に対するご理解の一助になれば，望外の幸せである。

＜謝　辞＞
筆者らの研究は，日本学術振興会（JSPS）の最先端研究開発支援プログラム，科学技術振興機構（JST）の再生医療実現拠点ネットワークプログラム「iPS細胞研究中核拠点」，および，厚生労働科学研究費補助金　難病・がん等の疾患分野の医療の実用化研究事業（再生医療関係研究分野）の助成によって行われた。

## 文　献

1) Takahashi, K. and Yamanaka, S. : Induction of pluripotent stem cells from mouse embryonic and adult fibroblast cultures by defined factors. Cell, 126 : 663～676, 2006.
2) Takahashi, K., Tanabe, K., Ohnuki, M., Narita, M., Ichisaka, T., Tomoda, K. and Yamanaka, S. : Induction of pluripotent stem cells from adult human fibroblasts by defined factors. Cell, 131 : 861～872, 2007.
3) Gurdon, J. B., Elsdale, T. R. and Fischberg, M. : Sexually mature individuals of Xenopus laevis from the transplantation of single somatic nuclei. Nature, 182 : 64～65, 1958.
4) Tada, M., Takahama, Y., Abe, K., Nakatsuji, N. and Tada, T. : Nuclear reprogramming of somatic cells by in vitro hybridization with ES cells. Curr. Biol., 11 : 1553～1558, 2001.
5) Thomson, J. A., Itskovitz-Eldor, J., Shapiro, S. S., Waknitz, M. A., Swiergiel, J. J., Marshall, V. S. and Jones, J. M. : Embryonic stem cell lines derived from human blastocysts. Science, 282 : 1145～1147, 1998.
6) Zhao, T., Zhang, Z. N., Rong, Z. and Xu, Y. : Immunogenicity of induced pluripotent stem cells. Nature, 474 : 212～215, 2011.
7) Araki, R., Uda, M., Hoki, Y., Sunayama, M., Nakamura, M., Ando, S., Sugiura, M., Ideno, H., Shimada, A., Nifuji, A. and Abe, M. : Negligible immunogenicity of terminally differentiated cells derived from induced pluripotent or embryonic stem cells. Nature, 494 : 100～104, 2013.
8) Morizane, A., Doi, D., Kikuchi, T., Okita, K., Hotta, A., Kawasaki, T., Hayashi, T., Onoe, H., Shiina, T., Yamanaka, S. and Takahashi, J. : Direct comparison of autologous and allogeneic transplantation of iPSC-derived neural cells in the brain of a nonhuman primate. Stem. Cell Reports, 1 : 283～292, 2013.
9) Nakagawa, M., Koyanagi, M., Tanabe, K., Takahashi, K., Ichisaka, T., Aoi, T., Okita, K., Mochiduki, Y., Takizawa, N. and Yamanaka, S. : Generation of induced pluripotent stem cells without Myc from mouse and human fibroblasts. Nat. Biotechnol., 26 : 101～106, 2008.
10) Nakagawa, M., Takizawa, N., Narita, M., Ichisaka, T. and Yamanaka, S. : Promotion of direct reprogramming by transformation-deficient Myc. Proc. Natl. Acad. Sci. U. S. A., 107 : 14152～14157, 2010.
11) Maekawa, M., Yamaguchi, K., Nakamura, T., Shibukawa, R., Kodanaka, I., Ichisaka, T., Kawamura, Y., Mochizuki, H., Goshima, N. and Yamanaka, S. : Direct reprogramming of somatic cells is promoted by maternal transcription factor Glis1. Nature, 474 : 225～229, 2011.
12) Huangfu, D., Osafune, K., Maehr, R., Guo, W., Eijkelenboom, A., Chen, S., Muhlestein, W. and Melton, D. A. : Induction of pluripotent stem cells from primary human fibroblasts with only Oct4 and Sox2. Nat. Biotechnol., 26 : 1269～1275, 2008.
13) Shi, Y., Desponts, C., Do, J. T., Hahm, H. S., Schöler, H. R. and Ding, S. : Induction of pluripotent stem cells from mouse embryonic fibroblasts by Oct4 and Klf4 with small-molecule compounds. Cell Stem Cell, 3 : 568～574, 2008.
14) Marshall, E. : Clinical research : Gene therapy a suspect in leukemia-like disease. Science, 298 : 34～35, 2002.
15) Fusaki, N., Ban, H., Nishiyama, A., Saeki, K. and Hasegawa, M. : Efficient induction of transgene-free human pluripotent stem cells using a vector based on Sendai virus, an RNA virus that does not integrate into the host genome. Proc. Jpn. Acad. Ser. B Phys. Biol. Sci., 85 : 348～362, 2009.
16) Okita, K., Matsumura, Y., Sato, Y., Okada, A., Morizane, A., Okamoto, S., Hong, H., Nakagawa, M., Tanabe, K., Tezuka, K., Shibata, T., Kunisada, T., Takahashi, M., Takahashi, J., Saji, H. and Yamanaka, S. : A more efficient method to generate integration-free human iPS cells. Nat. Methods, 8 : 409～412, 2011.
17) Warren, L., Manos, P. D., Ahfeldt, T., Loh, Y. H., Li, H., Lau, F., Ebina, W., Mandal, P. K., Smith, Z. D., Meissner, A., Daley, G. Q., Brack, A. S., Collins, J. J., Cowan, C., Schlaeger, T. M. and Rossi, D. J. : Highly efficient reprogramming to pluripotency and directed differentiation of human cells with synthetic modified mRNA. Cell Stem Cell, 7 : 618～630, 2010.
18) Miyoshi, N., Ishii, H., Nagano, H., Haraguchi, N., Dewi, D. L., Kano, Y., Nishikawa, S., Tanemura, M., Mimori, K., Tanaka, F., Saito, T., Nishimura, J., Takemasa, I., Mizushima, T., Ikeda, M., Yamamoto, H., Sekimoto, M., Doki, Y. and Mori, M. : Reprogramming of mouse and human cells to pluripotency using mature microRNAs. Cell Stem Cell, 8 : 633～638, 2011.
19) Rodríguez-Pizà, I., Richaud-Patin, Y., Vassena, R., González, F., Barrero, M. J., Veiga, A., Raya, A. and Izpisúa Belmonte, J. C. : Reprogramming of human fibroblasts to induced pluripotent stem cells under xeno-free conditions. Stem Cells, 28 : 36～44, 2010.
20) Doi, D., Samata, B., Katsukawa, M., Kikuchi, T., Morizane, A., Ono, Y., Sekiguchi, K., Nakagawa, M., Parmar, M. and Takahashi, J. : Isolation of human induced plu-

ripotent stem cell-derived dopaminergic progenitors by cell sorting for successful transplantation. Stem Cell Reports, 2：337～350, 2014.
21) 日本移植学会：臓器移植ファクトブック2013. http://www.asas.or.jp/jst/pdf/factbook/factbook2013.pdf
22) Han, S., Bourdon, A., Hamou, W., Dziedzic, N., Goldman, O. and Gouon-Evans, V.：Generation of functional hepatic cells from pluripotent stem cells. J. Stem Cell Res. Ther., S10：008, 2012.
23) Espejel, S., Roll, G. R., McLaughlin, K. J., Lee, A. Y., Zhang, J. Y., Laird, D. J., Okita, K., Yamanaka, S. and Willenbring, H.：Induced pluripotent stem cell-derived hepatocytes have the functional and proliferative capabilities needed for liver regeneration in mice. J Clin Invest., 120：3120～3126, 2010.
24) Takebe, T., Sekine, K., Enomura, M., Koike, H., Kimura, M., Ogaeri, T., Zhang, R. R., Ueno, Y., Zheng, Y. W., Koike, N., Aoyama, S., Adachi, Y. and Taniguchi, H.：Vascularized and functional human liver from an iPSC-derived organ bud transplant. Nature, 499：481～484, 2013.
25) Yusa, K., Rashid, S. T., Strick-Marchand, H., Varela, I., Liu, P. Q., Paschon, D. E., Miranda, E., Ordóñez, A., Hannan, N. R., Rouhani, F. J., Darche, S., Alexander, G., Marciniak, S. J., Fusaki, N., Hasegawa, M., Holmes, M. C., Di, Santo, J. P., Lomas, D. A., Bradley, A. and Vallier, L.：Targeted gene correction of α1 antitrypsin deficiency in induced pluripotent stem cells. Nature, 478：391～394, 2011.
26) 日本糖尿病学会編：科学的根拠に基づく糖尿病診療ガイドライン2013, 南江堂, 東京, 2013.
27) Nostro, M. C., Sarangi, F., Ogawa, S., Holtzinger, A., Corneo, B., Li, X., Micallef, S. J., Park, I. H., Basford, C., Wheeler, M. B., Daley, G. Q., Elefanty, A. G., Stanley, E. G. and Keller, G.：Stage-specific signaling through TGFβ family members and WNT regulates patterning and pancreatic specification of human pluripotent stem cells. Development, 138：861～871, 2011.
28) Tateishi, K., He, J., Taranova, O., Liang, G., D'Alessio, A. C. and Zhang, Y.：Generation of insulin-secreting islet-like clusters from human skin fibroblasts. J. Biol. Chem., 283：31601～31607, 2008.
29) Kroon, E., Martinson, L. A., Kadoya, K., Bang, A. G., Kelly, O. G., Eliazer, S., Young, H., Richardson, M., Smart, N. G., Cunningham, J., Agulnick, A. D., D'Amour, K. A., Carpenter, M. K. and Baetge, E. E.：Pancreatic endoderm derived from human embryonic stem cells generates glucose-responsive insulin-secreting cells in vivo. Nat. Biotechnol., 26：443～452, 2008.
30) Rezania, A., Bruin, J. E., Riedel, M. J., Mojibian, M., Asadi, A., Xu, J., Gauvin, R., Narayan, K., Karanu, F., O'Neil, J. J., Ao, Z., Warnock, G. L. and Kieffer, T. J.：Maturation of human embryonic stem cell-derived pancreatic progenitors into functional islets capable of treating pre-existing diabetes in mice. Diabetes, 61：2016～2029, 2012.
31) Kobayashi, T., Yamaguchi, T., Hamanaka, S., Kato-Itoh, M., Yamazaki, Y., Ibata, M., Sato, H., Lee, Y. S., Usui, J., Knisely, A. S., Hirabayashi, M. and Nakauchi, H.：Generation of rat pancreas in mouse by interspecific blastocyst injection of pluripotent stem cells. Cell, 142：787～799, 2010.
32) Matsunari, H., Nagashima, H., Watanabe, M., Umeyama, K., Nakano, K., Nagaya, M., Kobayashi, T., Yamaguchi, T., Sumazaki, R., Herzenberg, L. A. and Nakauchi, H.：Blastocyst complementation generates exogenic pancreas in vivo in apancreatic cloned pigs. Proc. Natl. Acad. Sci. U. S. A., 110：4557～4562, 2013.
33) Sato, T., Vries, R. G., Snippert, H. J., van de Wetering, M., Barker, N., Stange, D. E., van Es, J. H., Abo, A., Kujala, P., Peters, P. J. and Clevers, H.：Single Lgr5 stem cells build crypt-villus structures in vitro without a mesenchymal niche. Nature, 459：262～265, 2009.
34) Spence, J. R., Mayhew, C. N., Rankin, S. A., Kuhar, M. F., Vallance, J. E., Tolle, K., Hoskins, E. E., Kalinichenko, V. V., Wells, S. I., Zorn, A. M., Shroyer, N. F. and Wells, J. M.：Directed differentiation of human pluripotent stem cells into intestinal tissue in vitro. Nature, 470：105～109, 2011.
35) Waddington, C. H.：The Strategy of the Genes. Geo Allen & Unwin, London, 1957.
36) Kajiwara, M., Aoi, T., Okita, K., Takahashi, R., Inoue, H., Takayama, N., Endo, H., Eto, K., Toguchida, J., Uemoto, S. and Yamanaka, S.：Donor-dependent variations in hepatic differentiation from human-induced pluripotent stem cells. Proc. Natl. Acad. Sci. U. S. A., 109：12538～12543, 2012.
37) Kunisada, Y., Tsubooka-Yamazoe, N., Shoji, M. and Hosoya, M.：Small molecules induce efficient differentiation into insulin-producing cells from human induced pluripotent stem cells. Stem Cell Res., 8：274～284, 2012.
38) 長船健二著：もっとよくわかる！幹細胞と再生医療, 羊土社, 東京, 2014.
39) 梅澤明弘, 笹井芳樹, 洪 実編：再生医療を実現化する幹細胞のメディカルサイエンス, 羊土社, 東京, 2012.

SCIENTIFIC REPORTS

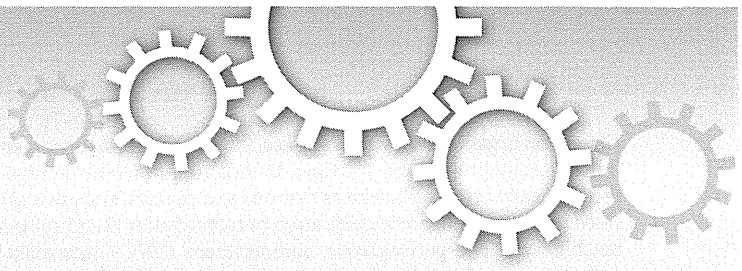

OPEN

SUBJECT AREAS:
INDUCED PLURIPOTENT STEM CELLS
IMAGE PROCESSING
NUCLEAR ORGANIZATION

Received
19 June 2014

Accepted
22 October 2014

Published
11 November 2014

Correspondence and requests for materials should be addressed to N.S. (norikos@kumamoto-u.ac.jp) or M.N. (mnakao@gpo.kumamoto-u.ac.jp)

# Computational image analysis of colony and nuclear morphology to evaluate human induced pluripotent stem cells

Kazuaki Tokunaga[1,2], Noriko Saitoh[1,2], Ilya G. Goldberg[3], Chiyomi Sakamoto[1], Yoko Yasuda[1], Yoshinori Yoshida[4], Shinya Yamanaka[4,5] & Mitsuyoshi Nakao[1,2]

[1]Department of Medical Cell Biology, Institute of Molecular Embryology and Genetics, Kumamoto University, 2-2-1 Honjo, Chuo-ku, Kumamoto 860-0811, Japan, [2]Core Research for Evolutional Science and Technology (CREST), Japan Science and Technology Agency, Tokyo, Japan, [3]Image Informatics and Computational Biology Unit, Laboratory of Genetics, National Institute on Aging, National Institutes of Health, 251 Bayview Boulevard, Suite 100, Baltimore, MD 21224, USA, [4]Center for iPS Cell Research and Application, Kyoto University, 53 Shogoin-Kawaharacho, Sakyo-ku, Kyoto, 606-8507, Japan, [5]Gladstone Institute of Cardiovascular Disease, 1650 Owens Street, San Francisco, CA 94158, USA.

**Non-invasive evaluation of cell reprogramming by advanced image analysis is required to maintain the quality of cells intended for regenerative medicine. Here, we constructed living and unlabelled colony image libraries of various human induced pluripotent stem cell (iPSC) lines for supervised machine learning pattern recognition to accurately distinguish bona fide iPSCs from improperly reprogrammed cells. Furthermore, we found that image features for efficient discrimination reside in cellular components. In fact, extensive analysis of nuclear morphologies revealed dynamic and characteristic signatures, including the linear form of the promyelocytic leukaemia (PML)-defined structure in iPSCs, which was reversed to a regular sphere upon differentiation. Our data revealed that iPSCs have a markedly different overall nuclear architecture that may contribute to highly accurate discrimination based on the cell reprogramming status.**

The generation of human induced pluripotent stem cells (iPSCs) is simple and highly reproducible[1]. However, only a small proportion of cells become pluripotent after introduction of the reprogramming factors, possibly resulting in a mixture of bona fide iPSCs and partially reprogrammed cells[2,3]. It is essential to develop reliable methods to select completely reprogrammed iPSCs by eliminating the contamination of non-iPSCs[4]. Previous studies have shown changes in gene expression, DNA methylation, and histone modifications during iPSC reprogramming[1,5]. Furthermore, reporter genes have been integrated into the genomic loci of pluripotency genes to visualize bona fide iPSCs[4]. However, there are no non-invasive methods that reliably identify live human iPSCs in large and heterogeneous populations of reprogramming cells.

Recent advances in automated biological image analyses enable objective measurements of cellular morphologies[6]. A supervised machine learning algorithm, wndchrm (weighted neighbour distances using a compound hierarchy of algorithms representing morphology), has been developed for automated image classification and mining of image similarities or differences[7]. It is a flexible, multi-purpose image classifier that can be applied to a wide range of bio-image problems. Unlike conventional image analysis, where users are required to specify target morphologies, choose specific algorithms, and try different parameters depending on the imaging problem, wndchrm users define classes by providing example images for each class; completely reprogrammed cells or partially reprogrammed cells, for example. Once classes are defined, classifications and similarity measurements are performed automatically. As the first step of the classification, wndchrm computes a large set of image features for each image in the defined classes and then selects image features that are informative for discrimination of the groups and constructs a classifier in an automated fashion[6,7]. Next, the dataset is tested by multiple rounds of cross validation to measure classification accuracy (CA) as well as class similarity, which can be visualized with phylogenetic tree. The wndchrm algorithm has been successfully used for early detection of osteoarthritis[8], measurement of muscle decline with aging, sarcopenia[9], classification of malignant lymphoma[10], and many other applications[10].

Nuclear structure and function are closely linked to cellular reprogramming and epigenomic regulation[5]. During cell differentiation, nuclear structures are reconfigured dynamically. Previous studies have identified numerous distinct nuclear bodies[11–13]. For example, promyelocytic leukaemia (PML) nuclear bodies typically exist as small spheres of 0.3–1.0 μm in diameter, and are implicated in various cellular pathways including

chromatin organisation, viral response, DNA replication, repair, and transcriptional regulation[11,13]. Cajal Bodies are prominent in highly metabolically active cells such as neurons and cancers, and are implicated in the assembly or modification of transcriptional and splicing machinery[14]. The perinucleolar compartment (PNC) accumulates polypyrimidine tract binding protein[15] and several polymerase III RNAs, which appears in virtually all types of solid tumours[16]. These bodies have been studied intensively in somatic cells[11–13], but much less is known about them in human iPSCs[17].

Here, we established an accurate classification method to identify iPSCs using images of unlabelled live iPSC colonies. A combination of wndchrm and specific morphology quantification suggested that signals contributing to morphological discrepancies reside in nuclear sub-domains.

## Results

**Colony morphologies reflect proper reprogramming, which can be measured by pattern recognition.** To build image classifiers to differentiate variously reprogrammed human cells, we first collected phase contrast images of live colonies formed by standard iPSC lines (201B7 and 253G1)[2,3], newly generated iPSC lines (1H–4H), non-iPSC lines (15B2 and 2B7), and somatic cells (human mammary epithelial cells, HMECs) (Fig. 1a). 253G1 and 201B7 cells were the initially established iPSC lines that were generated from human fibroblasts by introduction of four factors (Oct3/4, Sox2, Klf4, and c-Myc) and three factors (Oct3/4, Sox2, and Klf4), respectively[2,3]. New iPSCs and non-iPSCs were derived from HMECs and human fibroblasts by a Sendai virus (SeV) carrying the four factors[18]. We confirmed that these iPSCs maintained pluripotency and could differentiate into three lineages *in vitro* (Supplementary Figs. S1 and S2)[2,3]. In contrast, 15B2 and 2B7 cells lacked pluripotency, probably because of failure to silence the transgenes and activate endogenous stemness genes[1]. The resultant image libraries included 60 colony images (1024 × 767 pixels) for each of the nine cell lines (Supplementary Fig. S3). In wndchrm, pattern recognition is based on ability to distinguish different classes, not pre-defined objects. Therefore, other than manually centering colonies, we used the entire colony image with no prior segmentation, as input.

The image classifier must be trained with a sufficient number of images. To optimize the classification capacities, we measured CA using different number of training data set of iPSC (1H) and non-iPSC (15B2), and found that the accuracy reached a plateau with more than 40 images (Supplementary Fig. S4a).

In addition, dividing a large image into multiple equal-sized tiles can sometimes provide better classification, particularly when numerous cells are distributed throughout an image. Treating the tilled images independently is expected to improve classification ability as the size of dataset increases[19,20]. Therefore, we measured CA with and without tiling and found that the accuracy was improved by breaking an image into more than 16 images (Supplementary Fig. S4b).

Under these optimized classification condition, we classified several cell lines against iPSCs (1H cells) and compared CAs (Fig. 1b). In this binary classification, CA reflects the degree of morphological dissimilarities[7]. If the morphologies of two cell types are very distinct, the classifier is expected to show higher rate of accurate cross validations, at the maximum CA of 1. 0. On the other hand, the CA value of random classification between two cell types with no feature differences is expected to be 0.5. The results showed that the CA against iPSCs (1H cells) was 0.66 for 2H cells, 0.68 for 201B7 cells, and 0.63 for 253G1 cells, but it was significantly high for non-iPSCs, 15B2 cells (0.87), and HMECs (0.96) (Fig. 1b). Therefore, wndchrm analysis was effective for discrimination of iPSC and non-iPSC colonies.

A set of informative image features extracted from each wndchrm test is summarized in Figure 1c and Supplementary Table S1. The Fisher discriminant values were clearly small between iPSC lines (1H vs. 2H, and 1H vs. 201B7), while they were remarkably large for non-iPSCs (15B2 cells) and HMECs that exhibited a common feature pattern (Fig. 1c). In addition, most of the image features that contributed to the accurate classifications were based on transformed images (Fig. 1c, black bars)[6,7]. Thus, wndchrm analyses are effective and objective for discrimination of iPSC and non-iPSC colonies.

We further examined the morphological similarities among the cell lines. The phylogeny in Fig. 1d was generated based on the pairwise class similarity (Supplementary Table S2), and showed that various iPSC lines, particularly those reprogrammed with the four factors, were closely clustered, whereas non-iPSCs (15B2) and HMECs were distantly positioned from them (Fig. 1d, and Supplementary Figs. S4c and S4d). A set of most informative image features extracted for this wndchrm test is listed in Supplementary Table S4.

Consistently, classifications between any combination of iPSC lines (1H-4H) resulted in low CA, which suggests that their morphologies are similar to each other (Supplementary Fig. S4e). Furthermore, binary classifications using another iPSC line (4H) as a reference (Supplementary Fig. S4f) resulted in a similar pattern to Fig. 1b.

Besides the above-mentioned studies on the cell lines, wndchrm analysis was effective to classify partially reprogrammed and fully reprogrammed mouse cells grown in the same dish as a mixed population (Supplementary Fig. S5).

Reprogrammed cells grow as large colonies. We investigated the nature of image features that discriminate iPSCs and non iPSCs. As mentioned above, we classified iPSCs (1H) and non-iPSCs (15B2) with and without tiling the colony images (Supplementary Fig. S4b). By doing so, an image is broken into equally sized rectangles that are treated independently for successive training and test. An important feature as a single entity is lost, while the one distributed throughout the image is maintained, and size of the data set increases. We found that the CA was improved by tiling (Supplementary Fig. S4b), suggesting that the signals to identify iPSCs (1H) and non-iPSCs (15B2) were scattered in the image, and the colony morphology *per se* is not critical.

We further localised image features that discriminate iPSCs (1H) and non-iPSC (15B2) by tiling the colony images into 64 tiles and measuring the CA in each of them (Fig. 1e). As expected, a large part of the predictive signal came from areas containing iPSCs. Interestingly, the higher signals (CA $\geq$ 0.75) were positioned inside of the colony region (Inside), rather than the periphery with the local edge shape (Periphery) or outside of the colony (MEF), suggesting that unique features of the internal structure of the colony contribute most to the distinction.

Because nuclear morphology changes during differentiation status[21–23], we searched nuclear sub-structures that are different in iPSCs and non-iPSCs. Among the nuclear structures tested in this study, lamin A/C, the major component of the nuclear lamina[24], was expressed in the peripheral cells of iPSC colonies, while it was detected in most of the cells in non-iPSC colonies (Fig. 1f). In addition, transcription factor Sp1 (specificity protein 1)[25] was highly expressed inside of iPSC colonies (Supplementary Fig. S6). Such a metastatic state of iPSCs in the colony may be recognized by wndchrm.

**The linear form of the PML-defined structure is characteristic of appropriately reprogrammed iPSCs.** Extensive immunofluorescence analyses of ~20 distinct nuclear structures revealed that the PML body[26,27], Cajal body[27], and PNC[27] were characteristic of bona fide iPSCs, non-iPSCs, and cancerous HeLa cells, respectively (Figs. 2a–b, and Supplementary Fig. S7). The frequency of PML body formation in iPSC lines (1H, 201B7, and 253G1) was less than that in non-iPSC lines (15B2 and 2B7), and somatic cell lines (HMECs and IMR90 fibroblasts). Cajal body formation in non-iPSCs (0 ± 0.2 per

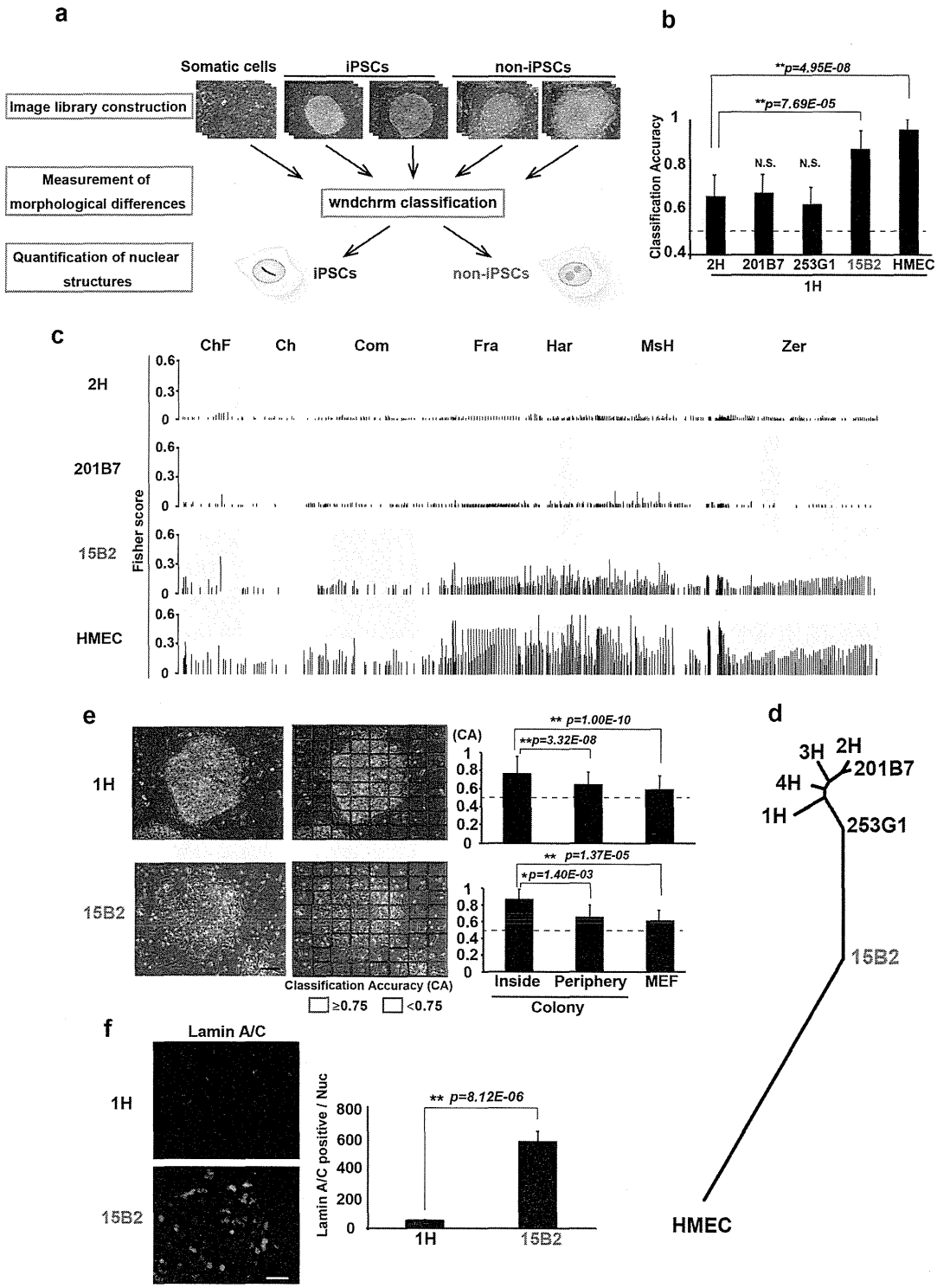


**Figure 1 | Quantitative classification of completely and incompletely reprogrammed human iPSC colonies.** (a) Experimental Overview. iPSCs and non-iPSCs are indicated as blue and red, respectively. (b) Binary classification of colony images against iPSCs (1H). Classification accuracy (CA) indicates the level of morphological differences between two cell types. CA value of two cell types with no feature differences is expected to be 0.5 (dotted line). The values are the means and standard deviation (s.d.) from 10 independent tests. N.S., not significant. (c) Fisher discriminant scores assigned to the 2873 features for each test in Fig. 1b. The values were calculated from raw (red bars) and transformed images (black bars). The name of each feature group is described in Supplementary Table S1. (d) Phylogeny based on morphological similarities. (e) Specification of the areas that distinguish iPSC (1H) and non-iPSC (15B2) colonies. CA values for each sub-image are shown as high (red) and low (blue). Average CA values inside, at the periphery, and outside of the colony (MEF, mouse embryonic fibroblast) are shown on the graph. (f) Selective expression of lamin A/C in the periphery of the iPSC colony. Immunofluorescence images of lamin A/C (green) and DAPI (blue), and quantified intensities are shown at the right (n>600). Values are the means and s.d. *, $p<0.05$; **, $p<0.01$. Scale bars, 200 μm.

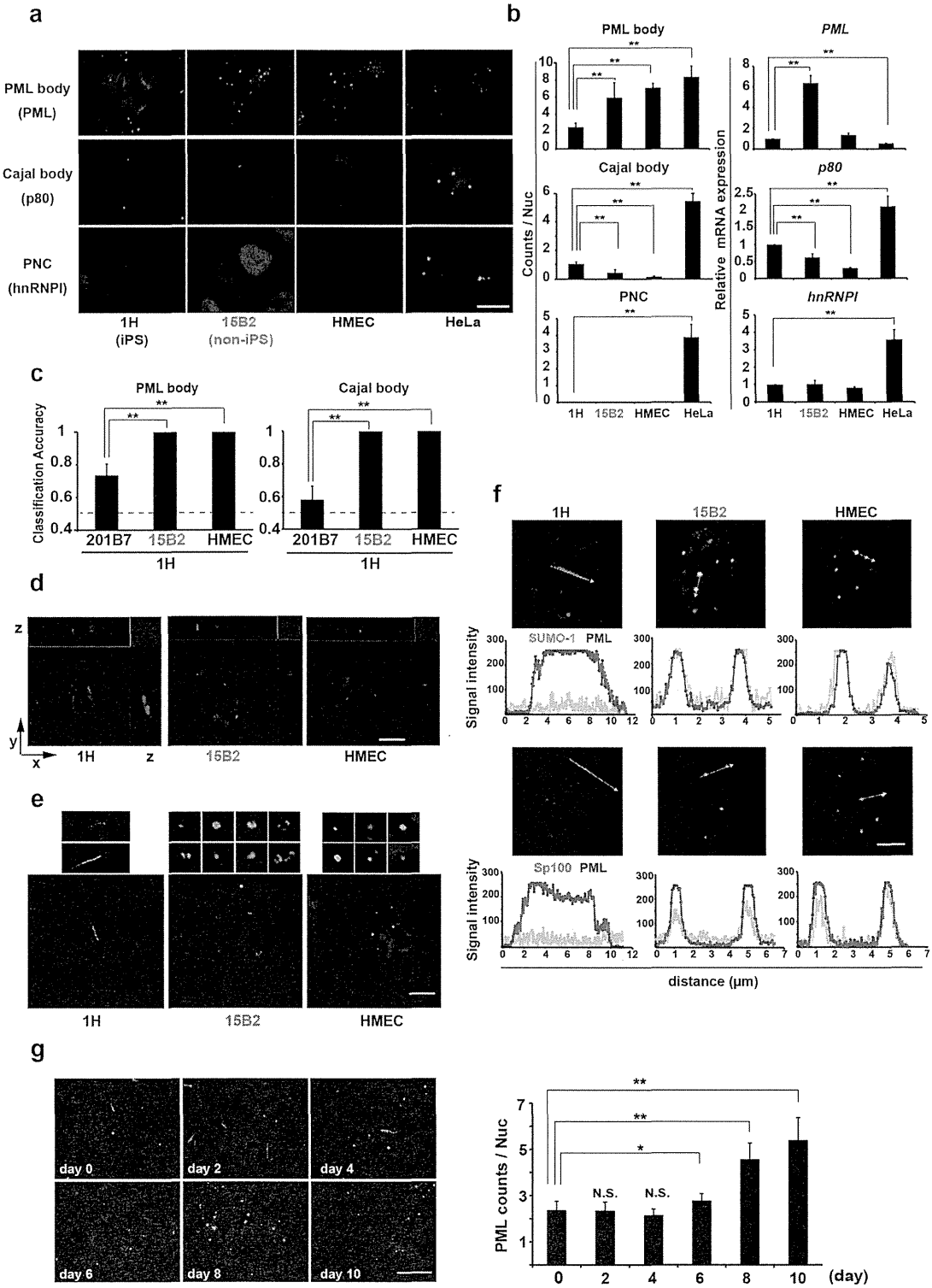


**Figure 2 | Quantitative assessment of nuclear structures in completely and incompletely reprogrammed human iPSCs.** (a) Identification of nuclear structure characteristics of iPSCs. Immunostaining was performed to identify the PML body (PML), Cajal body (p80 coilin), and perinucleolar compartment (PNC) (hnRNP I) (green). Nuclei were stained with DAPI (blue). (b) Quantification of nuclear structure formation (n>200, left) and the mRNA levels of the corresponding components in the structures (n=3, right). (c) wndchrm classifications against iPSCs (1H) using immunofluorescence images of PML and Cajal bodies (n=10). (d) Detection of linear PML structures by three-dimensional confocal microscopy. (e) Detection of PML structural variation by structured illumination microscopy (100 nm resolution). Enlarged images of PML structures are shown in the upper boxes. (f) Lack of SUMO-1 and Sp100 in the linear PML structures of bona fide iPSCs. The signal intensity along the arrow is shown below. PML, red; SUMO-1 and Sp100, green. (g) Transition of PML structures from linear to round during differentiation. The number of PML structures is shown at the right (n>300). Values are the means and s.d. *, $p<0.05$; **, $p<0.01$. Scale bars, 5 μm.

nucleus in 15B2 and 2B7 cells) and somatic cells (HMECs and IMR90 fibroblasts) was less frequent than that in iPSCs (1 ± 0.15 per nucleus in 1H, 201B7, and 253G1 cells), implying that hypoplasia of Cajal bodies is a feature of non-iPSCs. The PNC was only observed in HeLa cells (mean number = 4 ± 0.77), which is consistent with its specific appearance in cancerous cells[16] and high expression of one of its components, hnRNPI, in HeLa cells (Fig. 2a–b).

Using the wndchrm image libraries constructed from immunofluorescence of the PML and Cajal bodies (Supplementary Fig. S8), bona fide iPSCs (1H cells) were discriminated from non-iPSCs (15B2 cells) by extremely high CA values (~1.0) (Fig. 2c).

PML-defined structures in iPSCs were especially striking. Linear PML structures were found uniquely in bona fide iPSCs (Fig. 2a and Supplementary Fig. S7a). Three-dimensional imaging by confocal microscopy revealed approximately straight, rod-like PML structures traversing within the nuclei of iPSCs (Fig. 2d). In addition, more detailed structures visualized by structured illumination microscopy showed at least three classes of PML structures: linear and connected bead-like in iPSCs (1H), irregular ring-like in non-iPSCs (15B2), and normal spheres in HMECs (Fig. 2e). In terms of protein composition, the linear PML structure in bona fide iPSCs was distinct from that in somatic cells (Fig. 2f). In somatic cells such as HMECs, the PML protein and its SUMO modification are required for PML body formation and colocalisation with other components such as Sp100[26]. In contrast, the linear PML structure in iPSCs evidently lacked enrichment of SUMO-1 and Sp100. Finally, we found that the PML-defined structure in iPSCs transited to a somatic sphere PML body under differentiation conditions (day 6–10) in parallel with an increased number of the bodies (Fig. 2g). The resulting PML bodies coexisted with SUMO-1 and Sp100 on day 10 (Supplementary Fig. S9). Thus, the PML structure is dynamically regulated in iPSCs during their differentiation, indicating that the linear form of the PML body is one of the hallmarks of fully reprogrammed iPSCs.

In summary, we report the morphometric characteristics of human iPSCs by quantitative assessment of colony and nuclear structures.

## Discussion

In the present study, we developed a new non-invasive method to distinguish nascent reprogrammed iPSC and non-iPSC colonies based on their morphologies. Previously, mouse reprogramming studies have used reporters integrated into the genomic loci of pluripotency genes Fbx15, Oct4, or Nanog[28–30] to identify reprogrammed cells. However, there have been no methods to reliably identify human iPSCs in a population of fibroblasts and imperfectly reprogrammed cells without cell labelling[4]. Our analysis using a collection of cell lines including standard iPSC lines (201B7 and 253G1)[2,3], newly generated iPSC lines (1H–4H), non-iPSC lines (15B2 and 2B7), and somatic cells (human mammary epithelial cells, HMECs) demonstrated that wndchrm analysis is effective and objective for discrimination of iPSC and non-iPSC colonies.

Quantitative measurement of morphological differences can be very complex, and it is sometimes difficult to analyse only predefined features[6,7,9]. Therefore, we used a supervised machine learning system, wndchrm, which has been developed to automatically mine for morphological similarities in a wide variety of objects[7,9]. As the first step, wndchrm computes a large number of features of both raw images and ones processed for transformations including Fourier, Wavelet and Chebyshev. Total calculated feature numbers are 2873 at maximum, which are expected to cover general image features. They include polynominal decompositions, high contrast features, pixel statistics and textures, and so on[7,19]. Next, wndchrm selects an informative feature by rejecting noisy feature by using Fisher Linear Discriminant algorithm. The Fischer scores are also used as feature weights, so that less discriminating features have a reduced effect on the classifier. The classifier used is WND5 which is related to the k-nearest neighbors type, except that it uses a negative exponential in a weighted feature space rather than a simple linear distance equation. While the classification system is composed of several linear elements, it is not justified to characterize this system as somehow limited in the complexity of the feature relationships it can exploit. In fact, wndchrm outperforms over a dozen state of the art classifiers which are constructed as either general, problem specific, linear or non-linear programming[7,31]. Because the method used here is versatile and not limited to any particular type of cell or image, it would be applicable to classify cells in various states, providing that a sufficient numbers of images and their retrospective metadata is available.

In this study, we found image features that discriminate between iPSCs and non-iPSC (Fig. 1e) within colony components. It is interesting that the value of morphological similarity does not depend on the original cell types or reprogramming procedures. For example, 201B7, 253G1, and 15B2 cells were all derived from human fibroblasts, However, 201B7 cells were closely clustered with 1H–4H cells that were derived from HMECs, suggesting that the cells have lost their lineage identities with morphological features during reprogramming. It is also interesting that the morphologies of the two non-iPSC lines (15B2 and 2B7) were not only distinct from iPSCs, but also from each other, implying that they have failed reprogramming at different stages or for different reasons (Supplementary Fig. S4d).

Prior to the colony classifications, we analyzed the cell lines for their undifferentiated states and differentiation abilities to find that they formed relatively homogeneous colonies (Supplementary Figs S1 and S2). However, reprogrammed cells generally could form a colony that is composed of different types of cells. A question of how the classification technology works on the heterogeneous colonies remains to be investigated. It is of interest that tiling an image was effective to determine the source of the classification signal in cultured colonies (Fig. 1e) and cells[10]. It was also successfully applied to determine the location of the predictive osteoarthritis signal in X-Rays[32].

We found that nuclear structures changed during reprogramming dynamically and specifically. Using immunofluorescence images of the PML and Cajal bodies, bona fide iPSCs (1H cells) were discriminated from non-iPSCs (15B2 cells) by extremely high accuracy, almost 100% accuracy, with wndchrm (Fig. 2c). This result suggests that one can use the information on the different nuclear bodies to discriminate between cell types effectively.

Among the nuclear structures, the linear PML-defined structure is an attractive indicator that represents the reprogramming state of iPSCs. The linear form of PML bodies has been observed in human embryonic stem (ES) cells[33], but not in mouse ES cells, possibly because human ES cells correspond to mouse-derived epiblast stem cells[34,35]. The ring-shaped PML body found in human non-iPSCs may represent a transition state from somatic cells to iPSCs. Collectively, the linear PML structure is likely to be characteristic of the pluripotent state of human cells.

In conclusion, the present study indicates that the reprogramming states of live human iPSCs can be evaluated precisely by machine learning technologies for image analyses. This versatile method is applicable to other cell types, and may be valuable for quality control of cells intended for regenerative medicine, as well as for basic research. Our findings will also significantly advance our knowledge of the nuclear landscape of iPSCs.

## Methods

**Generation and maintenance of iPSC lines.** To generate human iPSC lines, four reprogramming factors (Oct3/4, Sox2, Klf4, and c-Myc) were introduced into HMECs and primary human fibroblasts using SeV vectors according to the manufacturer's protocol (Cyto tune-iPS DNAVEC). Briefly, $2 \times 10^5$ cells were plated and infected with SeV vectors, and then cultured in Dulbecco's modified Eagle's medium (DMEM) supplemented with 10% foetal bovine serum. After ES cell-like

colonies appeared, the medium was changed to primate ES cell medium supplemented with 5 ng/ml basic fibroblast growth factor (bFGF) (ReproCELL). Growing colonies were picked up mechanically, expanded, and maintained on mouse embryonic fibroblasts (MEFs) to avoid spontaneous differentiation. Standard human iPSC lines, 201B7 and 253G1, were provided by Kyoto University and RIKEN BioResource Center, Japan, respectively. These cell lines were cultured on MEFs in Repro Stem medium supplemented with 5 ng/ml bFGF and penicillin/streptomycin.

***In vitro* differentiation of human iPSCs.** For embryoid body (EB) formation, iPSCs were treated with a dissociation solution (CTK, ReproCELL), and clumps of cells were cultured in DMEM/F12 containing 20% knockout serum replacement (Invitrogen) supplemented with 9.2 mM L-glutamine, $1 \times 10^{-4}$ M non-essential amino acids, $1 \times 10^{-4}$ M 2-mercaptoethanol, and penicillin/streptomycin. The medium was changed every other day. After 8 days of floating culture, EBs were transferred to a gelatin-coated plate and cultured in the same medium for another 8 days.

**Immunofluorescence analysis.** Cells were fixed with 4% paraformaldehyde in PBS for 10 min at room temperature, washed, and permeabilized with PBS containing 0.5% Triton X-100 for 5 min on ice. The cells were then incubated with primary antibodies for 1 h, followed by secondary antibodies for 1 h. Images were obtained under a microscope (IX-71; Olympus) equipped with a 60 × NA1.0 Plan Apo objective lens and a cooled charged-coupled device camera (Hamamatsu). Alternatively, images were captured with a confocal laser-scanning microscope (LSM 710, Carl Zeiss) with a 63 ×/1.4 Plan-Apochromat objective lens and a cooled charged-coupled device camera (Carl Zeiss). For immunofluorescences of the nuclear structures (PML body, Cajal body and PNC), image stacks containing three-dimensional datasets were collected at 1.0 μm intervals through the z axis, and projected onto two dimensions using imaging software (Lumina Vision; Mitani Corp). For structured illumination microscopic analyses, we used a microscope (Ti-E; Nikon) equipped with a 100 × NA1.49 CFI Apo TIRF objective lens, an electron multiplying charged-coupled device camera (iXon Em-CCD, Andor), and image acquisition software (Nikon).

**Image quantification.** For image classifications, we used wndchrm ver. 1.31[6,7]. Images used were; phase contrast of colonies (1024 × 767 pixels) (Supplementary Fig. S3), and immunofluorescences of nuclear structures (1280 × 1024 pixels) (Supplementary Fig. S8). No further segmentation was done prior to wndchrm analysis. The numbers of training/test images were 60/6 (Fig. 1), 40/8 (PML body in Fig. 2), 35/7 (Cajal body in Fig. 2), and 26/7 (Supplementary Fig. S5). The options used were a larger feature set of 2873 (-l), tiling of an image into 4 (-t4) for Fig. 1b–1d, and (-l, -t8) for Fig. 1e. Fisher scores were automatically computed for each feature in the following groups: ChF, Chebyshev-Fourier Statistics; Ch, Chebyshev Statistics; Com, Combined First Fourier Moments; Fra, Edge and Fractal Statistics; Har, Haralick Texture; MsH, Multiscale Histogram; Zer, Zernike Moments (Fig. 1c and Supplementary Fig. S4c)[7]. Pairwise class similarity values in Supplementary Table S2 were computed from the average of the marginal probabilities of all of the test images in each class. The per-class marginal probabilities were used as coordinates in a marginal probability space, where pairwise inter-class distances were computed using the Euclidean distance formula. Morphological similarity is the inverse of morphological distance between classes. Phylogenies were computed using the Fitch-Margoliash method implemented in the PHYLIP package, which is based on pairwise class similarity values reported by wndchrm ver 1.3[9,36]. For imaging cytometry analyses, CELAVIEW RS100 (Olympus) was used to capture images, and quantitative analyses was done using CELAVIEW analysis software as following. For automated quantification of PML body, Cajal body and PNC, each fluorescent image was segmented in CELAVIEW (Olympus) using the DAPI channel to define the nuclei. The nuclear bodies were automatically segmented based on their intensity and area using CELAVIEW as previously reported[37].

**RNA isolation and quantitative PCR analysis.** Total RNA was isolated using TRIzol (Invitrogen). For cDNA synthesis, 1 μg of total RNA was reverse transcribed with a High Capacity cDNA Reverse Transcription Kit (Applied Biosystems). Quantitative PCR of target cDNAs was performed using Power SYBR Green PCR Master Mix (Applied Biosystems). Each experiment was performed at least three times. Relative fold changes were quantified by normalisation to *β-actin* expression. Primer sequences are listed in Supplementary Table S3.

**Antibodies.** The primary antibodies used were: mouse PML (1 : 500, SC-966, Santa Cruz), p80 coilin (1 : 300, #612074, BD Biosciences), hnRNPI (1 : 300, sc-16547, Santa Cruz), lamin A/C (1 : 300, sc-7292, Santa Cruz), Sp1 (1 : 300, sc-16547, Santa Cruz), and lamin B (1 : 300, sc-6216, Santa Cruz). The following secondary antibodies were used: Alexa 488-conjugated donkey anti-mouse IgG (1 : 250), Alexa 488-conjugated donkey anti-rabbit IgG (1 : 250) (Molecular Probes), Cy3-conjugated donkey anti-mouse IgG (1 : 1000), Cy3-conjugated donkey anti-rat IgG (1 : 1000), and Cy3-conjugated donkey anti-rabbit IgG (1 : 1000) (Jackson ImmunoResearch).


1. Yamanaka, S. & Blau, H. M. Nuclear reprogramming to a pluripotent state by three approaches. *Nature* **465**, 704–712 (2010).
2. Takahashi, K. *et al.* Induction of pluripotent stem cells from adult human fibroblasts by defined factors. *Cell* **131**, 861–872 (2007).
3. Nakagawa, M. *et al.* Generation of induced pluripotent stem cells without Myc from mouse and human fibroblasts. *Nat Biotechnol* **26**, 101–106 (2008).
4. Chan, E. M. *et al.* Live cell imaging distinguishes bona fide human iPS cells from partially reprogrammed cells. *Nat Biotechnol* **27**, 1033–1037 (2009).
5. Meissner, A. Epigenetic modifications in pluripotent and differentiated cells. *Nat Biotechnol* **28**, 1079–1088 (2010).
6. Eliceiri, K. W. *et al.* Biological imaging software tools. *Nat Methods* **9**, 697–710 (2012).
7. Orlov, N. *et al.* WND-CHARM: Multi-purpose image classification using compound image transforms. *Pattern Recog Lett* **29**, 1684–1693 (2008).
8. Grisendi, S. *et al.* Role of nucleophosmin in embryonic development and tumorigenesis. *Nature* **437**, 147–153 (2005).
9. Johnston, J., Iser, W. B., Chow, D. K., Goldberg, I. G. & Wolkow, C. A. Quantitative image analysis reveals distinct structural transitions during aging in Caenorhabditis elegans tissues. *PLoS One* **3**, e2821 (2008).
10. Shamir, L., Orlov, N., Mark Eckley, D., Macura, T. J. & Goldberg, I. G. IICBU 2008: a proposed benchmark suite for biological image analysis. *Med Biol Eng Comput* **46**, 943–947 (2008).
11. Scaglioni, P. P. *et al.* Translation-dependent mechanisms lead to PML upregulation and mediate oncogenic K-RAS-induced cellular senescence. *EMBO Mol Med* **4**, 594–602 (2012).
12. Zhao, R., Bodnar, M. S. & Spector, D. L. Nuclear neighborhoods and gene expression. *Curr Opin Genet Dev* **19**, 172–179 (2009).
13. Bernardi, R. & Pandolfi, P. P. Structure, dynamics and functions of promyelocytic leukaemia nuclear bodies. *Nat Rev Mol Cell Biol* **8**, 1006–1016 (2007).
14. Morris, G. E. The Cajal body. *Biochim Biophys Acta* **1783**, 2108–2115 (2008).
15. Ghetti, A., Pinol-Roma, S., Michael, W. M., Morandi, C. & Dreyfuss, G. hnRNP I, the polypyrimidine tract-binding protein: distinct nuclear localization and association with hnRNAs. *Nucleic Acids Res* **20**, 3671–3678 (1992).
16. Norton, J. T. & Huang, S. The perinucleolar compartment: RNA metabolism and cancer. *Cancer Treat Res* **158**, 139–152 (2013).
17. Fussner, E. *et al.* Constitutive heterochromatin reorganization during somatic cell reprogramming. *The EMBO Jl* **30**, 1778–1789 (2011).
18. Fusaki, N., Ban, H., Nishiyama, A., Saeki, K. & Hasegawa, M. Efficient induction of transgene-free human pluripotent stem cells using a vector based on Sendai virus, an RNA virus that does not integrate into the host genome. *Proc Jpn Acad Ser B Phys Biol Sci* **85**, 348–362 (2009).
19. Shamir, L. *et al.* Wndchrm - an open source utility for biological image analysis. *Source Code Biol Medicine* **3**, 13 (2008).
20. Shamir, L., Delaney, J. D., Orlov, N., Eckley, D. M. & Goldberg, I. G. Pattern recognition software and techniques for biological image analysis. *PLoS Comp Biol* **6**, e1000974 (2010).
21. Gasser, S. M. Visualizing chromatin dynamics in interphase nuclei. *Science* **296**, 1412–1416 (2002).
22. Meshorer, E. & Misteli, T. Chromatin in pluripotent embryonic stem cells and differentiation. *Nature reviews. Molec Cell Biol* **7**, 540–546 (2006).
23. Aoto, T., Saitoh, N., Ichimura, T., Niwa, H. & Nakao, M. Nuclear and chromatin reorganization in the MHC-Oct3/4 locus at developmental phases of embryonic stem cell differentiation. *Dev Biol* **298**, 354–367 (2006).
24. Constantinescu, D., Gray, H. L., Sammak, P. J., Schatten, G. P. & Csoka, A. B. Lamin A/C expression is a marker of mouse and human embryonic stem cell differentiation. *Stem Cells* **24**, 177–185 (2006).
25. Safe, S. & Abdelrahim, M. Sp transcription factor family and its role in cancer. *Eur J Cancer* **41**, 2438–2448 (2005).
26. Zhong, S., Salomoni, P. & Pandolfi, P. P. The transcriptional role of PML and the nuclear body. *Nat Cell Biol* **2**, E85–90 (2000).
27. Mao, Y. S., Zhang, B. & Spector, D. L. Biogenesis and function of nuclear bodies. *Trends Genet* **27**, 295–306 (2011).
28. Takahashi, K. & Yamanaka, S. Induction of pluripotent stem cells from mouse embryonic and adult fibroblast cultures by defined factors. *Cell* **126**, 663–676 (2006).
29. Okita, K., Ichisaka, T. & Yamanaka, S. Generation of germline-competent induced pluripotent stem cells. *Nature* **448**, 313–317 (2007).
30. Wernig, M. *et al.* In vitro reprogramming of fibroblasts into a pluripotent ES-cell-like state. *Nature* **448**, 318–324 (2007).
31. Orlov, N. V., Eckley, D. M., Shamir, L. & Goldberg, I. G. Improving class separability using extended pixel planes: a comparative study. *Machine Vis Applic* **23**, 1047–1058 (2012).
32. Shamir, L. *et al.* Early detection of radiographic knee osteoarthritis using computer-aided analysis. *Osteoarth Cartilage/OARS, Osteoarth Res Society* **17**, 1307–1312 (2009).
33. Butler, J. T., Hall, L. L., Smith, K. P. & Lawrence, J. B. Changing nuclear landscape and unique PML structures during early epigenetic transitions of human embryonic stem cells. *J Cell Biochem* **107**, 609–621 (2009).
34. Brons, I. G. *et al.* Derivation of pluripotent epiblast stem cells from mammalian embryos. *Nature* **448**, 191–195 (2007).
35. Tesar, P. J. *et al.* New cell lines from mouse epiblast share defining features with human embryonic stem cells. *Nature* **448**, 196–199 (2007).
36. Felsenstein, J. PHYLIP—Phylogeny Inference Package (Version 3.2). *Cladistics* **5**, 164–166 (1989).

37. Saitoh, N. *et al.* The distribution of phosphorylated SR proteins and alternative splicing are regulated by RANBP2. *Mol Biol Cell* **23**, 1115–1128 (2012).

## Acknowledgments

We thank Dr. Tamiyo Kobayashi (Olympus, Japan) for technical assistance. This work was supported by grants from the Ministry of Education, Culture, Sports, Science and Technology of Japan and the Japan Science and Technology Agency (CREST) (M.N. and N.S.).

## Author contributions

K.T., N.S. and M.N. designed and performed the experiments, and prepared the manuscript, together with I.G.G. for the wndchrm analyses, Y.Y. and S.Y. for the images of iPSC colonies, and C.S. and Y.Y. for technical assistance.

## Additional information

**Supplementary information** accompanies this paper at http://www.nature.com/scientificreports

**Competing financial interests:** S.Y. is a member without salary of the scientific advisory board of iPS Academia Japan. Y.Y. is a founder of iPS Portal.

**How to cite this article:** Tokunaga, K. *et al.* Computational image analysis of colony and nuclear morphology to evaluate human induced pluripotent stem cells. *Sci. Rep.* **4**, 6996; DOI:10.1038/srep06996 (2014).

This work is licensed under a Creative Commons Attribution-NonCommercial-NoDerivs 4.0 International License. The images or other third party material in this article are included in the article's Creative Commons license, unless indicated otherwise in the credit line; if the material is not included under the Creative Commons license, users will need to obtain permission from the license holder in order to reproduce the material. To view a copy of this license, visit http://creativecommons.org/licenses/by-nc-nd/4.0/

# iPS 細胞
iPS cells(induced Pluripotent Stem cells)

Related words リプログラミング，再生医療用 iPS 細胞ストック



## iPS 細胞の樹立

機能を失った組織を回復させ，患者の生命予後や QOL を高めるために再生医療への期待が高まっている．ES 細胞，iPS 細胞などの胚性幹細胞はその頑強な自己増殖能と分化多能性から再生医療の細胞ソースとして期待されている．

1962 年に Gurdon は，アフリカツメガエルにおいて体細胞核移植により体細胞を初期化できることを明らかにし[1]，その後，哺乳類においても体細胞核移植による細胞初期化は可能であることが明らかになった．一方で体細胞と ES 細胞との細胞融合によっても初期化が可能であることが明らかになり[2]，ES 細胞や卵が体細胞の初期化に必要な因子をもっていると考えられていた．高橋らは ES 細胞に特異的に発現する遺伝子のスクリーニングを行い，Oct3/4，Sox2，c-Myc および Klf4 の 4 因子を遺伝子導入・発現させることで，マウスの体細胞から多分化能をもつ細胞を樹立し，iPS 細胞(induced Pluripotent Stem Cell)と名づけた[3]．翌年には，ヒトの体細胞においても同様のリプログラミング因子の遺伝子導入により iPS 細胞の樹立に成功した[4]．当初，iPS 細胞は，レトロウイルスや，レンチウイルスによる遺伝子導入法で樹立されていたが，プラスミドベクターやセンダイウイルスなどのゲノム挿入のない遺伝子導入法によっても iPS 細胞樹立が可能になっている．

iPS 細胞誘導のリプログラミング過程においては，特定のシグナル経路がリプログラミングを抑制する障壁となることが知られている．腫瘍抑制蛋白である p53 のシグナル経路は代表的なリプログラミング障壁であり，p53 のノックダウンにより iPS 細胞誘導効率が上昇する．また最近，NuRD 複合体の構成要素である Mbd3 を抑制することによりリプログラミング効率が劇的に向上することが報告された[5]．

iPS 細胞はさまざまな種類の体細胞から樹立可能であり，一度に複数の iPS 細胞株が樹立可能である．しかし，これら複数のクローン間ではゲノム，エピゲノムの状態，細胞核初期化の程度，分化誘導時の分化しやすさなどが異なっている．そのため樹立した iPS 細胞クローンの品質の評価が重要と考えられる．

## iPS 細胞の再生医療への応用

再生医療における細胞ソースとして iPS 細胞より分化させた細胞を使用する場合に，未分化な細胞が残存して含まれていると奇形腫などの腫瘍が発生する可能性がある．マウスの iPS 細胞より分化誘導した神経細胞をマウスに移植する実験では，iPS 細胞の起源となる細胞種の違いにより未分化細胞の残存率および移植後の奇形腫形成率に違いがみられた[6]．この結果から神経分化誘導における分化抵抗性が細胞株によって違いがあると考えられる．また，ヒト iPS 細胞においても神経分化誘導において分化抵抗性 iPS 細胞株が存在しており，これらの分化抵抗性株においては，内在性レトロウイルス LTR7 関連遺伝子である HHLA1，ABHD12B，C4orf51 などの遺伝子の発現上昇が認められ，分化抵抗性株を選別するマーカーとなりうると考えられた[7]．このように iPS 細胞を用いた再生医療のためには適切な iPS 細胞株を選別することが重要であるが，分化抵抗性の有無は細胞の品質を評価するための重要な指標であると考えられる．

iPS 細胞の品質評価としてゲノムの安定性も重要な指標である．これまで ES/iPS 細胞は培養を続けるに従い，染色体異常，ゲノムコピー数変異，一塩基変異などが生じることが知られている．また，iPS 細胞はひとつの体

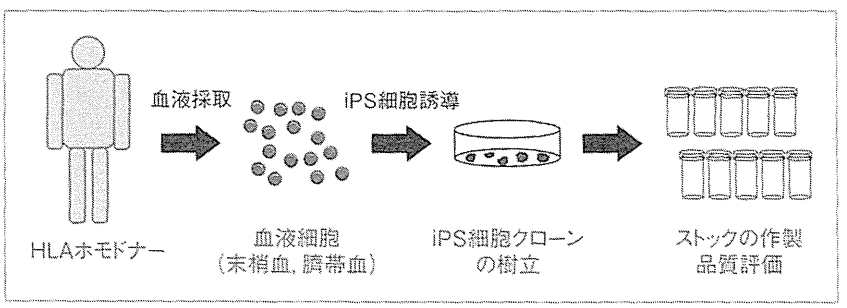


図 1　再生医療用 iPS 細胞ストック

細胞よりリプログラミング過程を経て樹立されるため，もともとの体細胞がもっていた変異(コピー数変異や一塩基変異)，およびリプログラミング過程での変異などが生じうるため，これらの変異の少ないiPS細胞株を選別する必要がある．

iPS細胞からの分化誘導においても，高効率で目的の細胞に分化誘導させることのできる技術の開発も重要である．さらに，目的の細胞に分化した細胞を選別する方法の開発も重要な課題と考えられる．発生学などのこれまでの知見に基づき，サイトカインや低分子化合物，培養条件の組合せにより神経細胞，心筋細胞，血液細胞などに分化誘導する定方向性分化誘導法が開発されており，これらの細胞を高効率に作製することが可能になってきている．また，抗体を用いたセルソーターによる細胞選別法など，目的の細胞を選別する方法も開発されている．心筋細胞を例にとれば，SIRPAやVCAM-1などの抗体による細胞選別法[8-10]，ミトコンドリア特異的蛍光色素[11]，無グルコース乳酸添加培地[12]による心筋細胞選択法など心筋細胞を純化する方法が報告されている．

## 再生医療用iPS細胞ストック(図1)

現在，京都大学において再生医療用iPS細胞ストックの整備が進められている．本プロジェクトは再生医療に使用できるGMP準拠のiPS細胞ストックを作製することを目的としている．HLA-A，BおよびDRの3座がホモのドナーより樹立したiPS細胞をストックすることによりHLA3座ホモの細胞50株で日本人の約73%，75株で80%をカバーすることが可能である[13]．この再生医療用iPS細胞ストックプロジェクトにより作製されたiPS細胞を用いて網膜色素上皮細胞，ドパミン産生ニューロン，血小板，心筋細胞，神経前駆細胞，角膜などの細胞移植治療の実現に向けた研究が進められている．

## おわりに

胚性幹細胞であるiPS細胞は，自己増殖能と分化多能性を併せもつため目的の細胞を大量に作製することが可能である．近年の分化誘導技術の発達や大量培養法の開発とともに，再生医療に応用可能な細胞を作製することが可能になりつつある．

再生医療用iPS細胞ストック整備やiPS細胞品質評価法も開発が進んでおり，iPS細胞を用いた再生医療の実現が期待される．




1) Gurdon, J. B.：*J. Embryol. Exp. Morphol.*, **10**：622, 1962.
2) Tada, M. et al.：*Curr. Biol.*, **11**：1553, 2001.
3) Takahashi, K. and Yamanaka, S.：*Cell*, **126**：663, 2006.
4) Takahashi, K. et al.：*Cell*, **131**：861, 2007.
5) Rais, Y. et al.：*Nature*, **502**：65, 2013.
6) Miura, K. et al.：*Nat. Biotechnol.*, **27**：743, 2009.
7) Koyanagi-Aoi, M. et al.：*Proc. Natl. Acad. Sci. USA*, 2013.
8) Dubois, N. C. et al.：*Nat. Biotechnol.*, **29**：p.1011：2011.
9) Uosaki, H. et al.：*PLoS One*, **6**：e23657, 2011.
10) Elliott, D. A. et al.：*Nat. Methods*, **8**：1037, 2011.
11) Hattori, F. et al.：*Nat. Methods*, **7**：61, 2010.
12) Tohyama, S. et al.：*Cell Stem Cell*, **12**：127, 2013.
13) Okita, K. et al.：*Nat. Methods*, **8**(5)：409, 2011.


■吉田善紀，山中伸弥／京都大学iPS細胞研究所初期化機構研究部門

# ES細胞とiPS細胞

吉田善紀
京都大学 iPS 細胞研究所

## はじめに

幹細胞生物学の発展とともに，これまで得ることが困難であったヒトの心筋細胞を作製することが可能になり，ヒト心筋細胞を再生医療や疾患研究，薬剤の毒性検査などに用いることが期待されるようになった．ES 細胞および iPS 細胞は体を構成するさまざまな細胞に分化することのできる分化多能性と，その分化多能性を維持しながら増殖することのできる自己増殖能を併せ持ち，その分化能と自己増殖能のために大量の分化細胞を作製することが可能であるため，ヒト心筋細胞を誘導する細胞ソースとして期待されている．ES 細胞は胚盤胞の状態の受精卵をフィーダー細胞と共培養することにより樹立されるが，患者自身の ES 細胞を樹立できないこと，樹立時に受精卵を滅失することなどの問題点がある．Oct3/4，Sox2，Klf4，c-Myc の 4 つの遺伝子を体細胞に導入することにより樹立される iPS 細胞は ES 細胞とほぼ同等の分化多能性と自己増殖能を持つとされている[1,2]．

## 定方向性心筋分化誘導法の開発

ヒトおよびマウスの多能性幹細胞は心筋や神経，血液細胞などのさまざまな細胞へ分化する能力を持つ．ES/iPS 細胞を凝集させ胚様体を形成することにより分化誘導が進み，血清存在下で拍動する心筋細胞を誘導することが可能であるが[3]，その分化誘導効率は低く一部の細胞が拍動する心筋細胞に分化する程度であった．しかし，再生医療や疾患研究などへの応用のためには，心筋細胞を高効率，高純度で分化誘導，純化させる方法の開発が必要である．そのため効率よく心筋細胞を分化誘導する定方向性分化誘導法が開発されてきた(図 1)．その 1 つの方法は分化誘導を支持する細胞との共培養系である．臓側内胚葉様細胞株の END-2 細胞を支持細胞とする共培養系において未分化な多能性幹細胞から心筋細胞を分化誘導することができることが報告されている[4,5]．胚様体形成法による分化誘導において血清非存在下で Activin A や BMP4 などのサイトカインを投与することにより胚様体は効率よく心筋に分化する[6]．またヒト ES/iPS 細胞単層培養系においても Activin A や BMP4 などのサイトカインによる刺激により心筋への分化誘導が可能であることが報告されている[7]．単層培養法による心筋分化誘導は基底膜マトリックス(マトリゲル)を培養皿底面にコートしさらに培養細胞上にオーバーレイする方法(matrix sandwich 法)により分化誘導効率が上昇することが知られている[8]．

## 心筋細胞分化を促進する因子の探索

心筋分化誘導効率を上昇させるような低分子化合物を探索するためのスクリーニングも施行されている．これまでに，アスコルビン酸，サイクロスポリン A，BMP シグナル阻害薬，Wnt シグナル阻害薬，p38MAPK 阻害薬などが心筋分化効率を促進することが報告されている[9~15]．これらの知見に基づき，サイトカインや血清を使用せず defined factor のみによって心筋分化誘導させることも可能になっている[15,16]．ES/iPS 細胞から心筋細胞を分化誘導するために必要とされる血清やサイトカインを低分子化合物で代用することができれば，コストの低減や細胞移植治療の際に動物由来成分を使用することによる

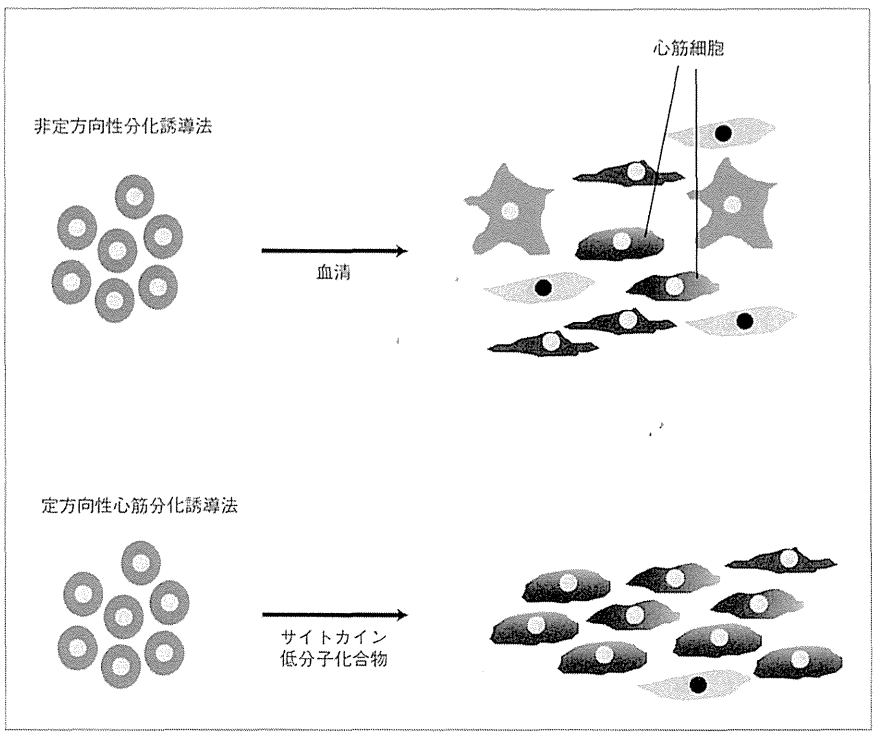


図1　サイトカインや低分子化合物を用いた定方向性心筋分化誘導法により高効率に心筋分化

感染症のリスクの回避などのメリットが期待できる.

### 心筋前駆細胞の同定と選別

心筋細胞分化誘導において，心筋細胞へ分化する能力を持つ心臓前駆細胞が出現するため，この心臓前駆細胞を同定し選別することができれば，高効率に心筋細胞へ分化する細胞として臨床応用への期待がされる．これまでに Flk-1, c-Kit, Isl-1 などの遺伝子が，心筋細胞，血管内皮細胞，平滑筋細胞などの細胞に分化する前駆細胞のマーカーであることが知られており，ヒト多能性幹細胞からの心筋分化誘導系において KDR 低発現，c-Kit 陽性の心臓前駆細胞を選別することにより効率よく心筋細胞が誘導されることが報告されている[6].

### 多能性幹細胞株間の心筋分化能

ヒト ES/iPS 細胞は細胞株間で分化指向性が異なることが知られている[17]．そのため同一の分化誘導プロトコールを適用しても細胞株によって目的の細胞に分化する程度が異なる(図 2)．この分化指向性の原因は十分には解明されていないが，定方向性分化誘導においては目的の細胞へ分化させるために要するサイトカイン(Activin A, BMP4 など)の濃度・期間が細胞株によって異なっている[18]．そのため，現状では細胞株ごとに分化誘導条件の最適化が必要であり，疾患特異的 iPS 細胞研究など細胞株間での比較が必要な解析においては分化心筋細胞の比較をするうえでの障壁となりうる.

### 分化心筋細胞の成熟

分化誘導系において誘導される心筋細胞はサルコ

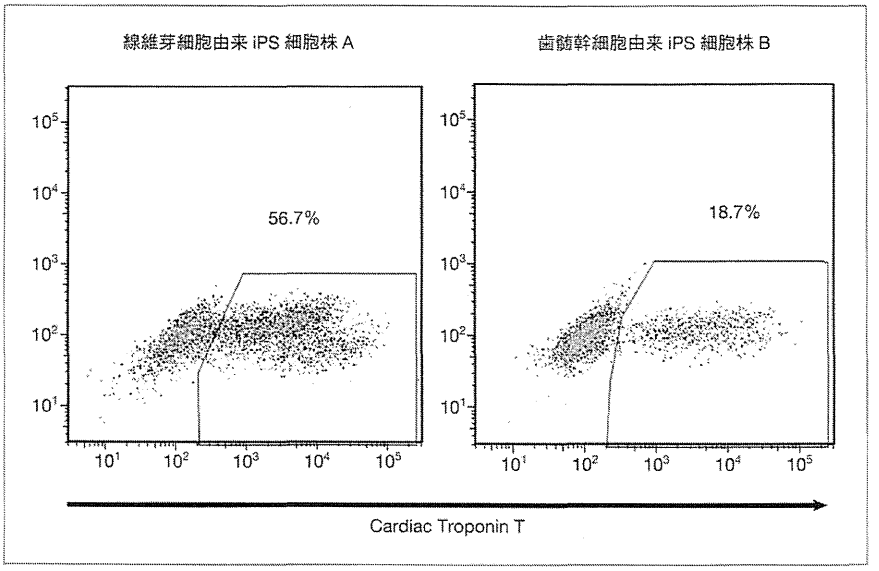


**図2　ヒト iPS 細胞株間の心筋分化能の違い**
同一プロトコール，サイトカイン濃度にて心筋分化能を比較した．

メア構造など形態的に成人の心臓組織の心筋細胞と比べると未熟であり，胎児心筋に近いとされている．また電気生理学的にも静止膜電位が高いなど成人心臓組織の心筋と比べて未熟な心筋の表現型を呈している．われわれは *in vitro* で長期培養を行うことによりサルコメア構造の成熟が認められることを報告した[19]．疾患研究や薬剤毒性検査などの目的には成人に近い成熟した心筋細胞のほうが適していると考えられるため，さらに成熟した心筋細胞を誘導する方法の開発が望まれる．

## 結語

定方向性分化誘導法の開発により高効率で心筋細胞を分化誘導する技術は発展してきており，細胞株間の分化指向性の違いの問題や分化心筋細胞の成熟など今後解決すべき問題はあるものの，高純度で大量の心筋細胞を作製することが可能になってきている．今後これらの細胞を用いることにより再生医療や心疾患研究のさらなる発展が期待される．

## 文　献

1) Takahashi K, Yamanaka S：Induction of pluripotent stem cells from mouse embryonic and adult fibroblast cultures by defined factors. *Cell* 2006；**126**(4)：663-676
2) Takahashi K, et al：Induction of pluripotent stem cells from adult human fibroblasts by defined factors *Cell* 2007；**131**(5)：861-872
3) Kehat I, et al：Human embryonic stem cells can differentiate into myocytes with structural and functional properties of cardiomyocytes. *J Clin Invest* 2001；**108**(3)：407-414
4) Mummery C, et al：Cardiomyocyte differentiation of mouse and human embryonic stem cells. *J Anat* 2002；**200**(Pt 3)：233-242
5) Mummery C, et al：Differentiation of human embryonic stem cells to cardiomyocytes：role of coculture with visceral endoderm-like cells. *Circulation* 2003；**107**(21)：2733-2740
6) Yang L, et al：Human cardiovascular progenitor cells develop from a KDR+ embryonic-stem-cell-derived population. *Nature* 2008；**453**(7194)：524-528
7) Laflamme MA, et al：Cardiomyocytes derived from human embryonic stem cells in pro-survival factors enhance function of infarcted rat hearts. *Nat Biotechnol* 2007；**25**(9)：1015-1024
8) Zhang J, et al：Extracellular matrix promotes highly efficient cardiac differentiation of human pluripotent stem cells：the matrix sandwich method. *Circ Res* 2012；**111**(9)：1125-1136
9) Takahashi T, et al：Ascorbic acid enhances differentia-

tion of embryonic stem cells into cardiac myocytes. *Circulation* 2003 ; **107**(14) : 1912-1916
10) Yan P, et al : Cyclosporin-A potently induces highly cardiogenic progenitors from embryonic stem cells. *Biochem Biophys Res Commun* 2009 ; **379**(1) : 115-120
11) Graichen R, et al : Enhanced cardiomyogenesis of human embryonic stem cells by a small molecular inhibitor of p38 MAPK. *Differentiation* 2008 ; **76**(4) : 357-370
12) Hao J, et al : Dorsomorphin, a selective small molecule inhibitor of BMP signaling, promotes cardiomyogenesis in embryonic stem cells. *PLoS One* 2008 ; **3**(8) : e2904,
13) Ren Y, et al : Small molecule Wnt inhibitors enhance the efficiency of BMP-4-directed cardiac differentiation of human pluripotent stem cells. *J Mol Cell Cardiol* 2011 ; **51**(3) : 280-287
14) Willems E, et al : Small-molecule inhibitors of the Wnt pathway potently promote cardiomyocytes from human embryonic stem cell-derived mesoderm. *Circ Res* 2011 ; **109**(4) : 360-364
15) Minami I, et al : A small molecule that promotes cardiac differentiation of human pluripotent stem cells under defined, cytokine- and xeno-free conditions. *Cell Rep* 2012 ; **2**(5) : 1448-1460
16) Burridge PW, et al : Chemically defined generation of human cardiomyocytes. *Nat Methods* 2014 ; **11**(8) : 855-860
17) Osafune K, et al : Marked differences in differentiation propensity among human embryonic stem cell lines. *Nat Biotechnol* 2008 ; **26**(3) : 313-315
18) Kattman SJ, et al : Stage-specific optimization of activin/nodal and BMP signaling promotes cardiac differentiation of mouse and human pluripotent stem cell lines. *Cell Stem Cell* 2011 ; **8**(2) : 228-240
19) Kamakura T, et al : Ultrastructural maturation of human-induced pluripotent stem cell-derived cardiomyocytes in a long-term culture. *Circ J* 2013 ; **77**(5) : 1307-1314

PLOS | ONE

RESEARCH ARTICLE

# Derivation of Mesenchymal Stromal Cells from Pluripotent Stem Cells through a Neural Crest Lineage using Small Molecule Compounds with Defined Media

**Makoto Fukuta[1,2,3☯], Yoshinori Nakai[4☯], Kosuke Kirino[5☯], Masato Nakagawa[6], Kazuya Sekiguchi[1,2,7], Sanae Nagata[2], Yoshihisa Matsumoto[1,2,3], Takuya Yamamoto[6,8], Katsutsugu Umeda[9], Toshio Heike[9], Naoki Okumura[10], Noriko Koizumi[10], Takahiko Sato[4], Tatsutoshi Nakahata[5], Megumu Saito[5], Takanobu Otsuka[3], Shigeru Kinoshita[4], Morio Ueno[4]*, Makoto Ikeya[2]*, Junya Toguchida[1,2,7]***

**1.** Department of Tissue Regeneration, Institute for Frontier Medical Sciences, Kyoto University, Kyoto, Japan, **2.** Department of Cell Growth and Differentiation, Center for iPS Cell Research and Application, Kyoto University, Kyoto, Japan, **3.** Department of Orthopaedic Surgery, Graduate School of Medical Sciences, Nagoya City University, Nagoya, Japan, **4.** Department of Ophthalmology, Kyoto Prefectural University of Medicine, Kyoto, Japan, **5.** Department of Clinical Application, Center for iPS Cell Research and Application, Kyoto University, Kyoto, Japan, **6.** Department of Reprogramming Science, Center for iPS Cell Research and Application, Kyoto University, Kyoto, Japan, **7.** Department of Orthopaedic Surgery, Graduate School of Medicine, Kyoto University, Kyoto, Japan, **8.** Institute for Integrated Cell-Material Sciences (WPI-iCeMS), Kyoto University, Kyoto, Japan, **9.** Department of Pediatrics, Graduate School of Medicine, Kyoto University, Kyoto, Japan, **10.** Department of Biomedical Engineering, Faculty of Life and Medical Sciences, Doshisha University, Kyotanabe, Japan

*mueno@koto.kpu-m.ac.jp (MU); mikeya@cira.kyoto-u.ac.jp (MI); togjun@frontier.kyoto-u.ac.jp (JT)

☯ These authors contributed equally to this work.

CrossMark
click for updates

OPEN ACCESS

**Citation:** Fukuta M, Nakai Y, Kirino K, Nakagawa M, Sekiguchi K, et al. (2014) Derivation of Mesenchymal Stromal Cells from Pluripotent Stem Cells through a Neural Crest Lineage using Small Molecule Compounds with Defined Media. PLoS ONE 9(12): e112291. doi:10.1371/journal.pone.0112291

**Editor:** Maurilio Sampaolesi, Stem Cell Research Institute, Belgium

**Received:** March 24, 2014

**Accepted:** October 6, 2014

**Published:** December 2, 2014

**Copyright:** © 2014 Fukuta et al. This is an open-access article distributed under the terms of the Creative Commons Attribution License, which permits unrestricted use, distribution, and reproduction in any medium, provided the original author and source are credited.

**Funding:** This work was supported in part by Grants-in-Aid for Scientific Research from JSPS (#25293320), a grant from Core Center for iPS Cell Research, Research Center Network for Realization of Regenerative Medicine from JST, and the Leading Project for Realization of Regenerative Medicine from MEXT to MI and JT. MI was also supported by the Adaptable and Seamless Technology Transfer Program through target-driven R&D, Exploratory Research from JST (AS242Z00931P). JT was also supported by the Center for Clinical Application Research on Specific Disease/Organ from JST. MU was also supported by Grants-in-Aid for Scientific Research from JSPS (#20791288). The funders had no role in the study design, data collection and analysis, decision to publish, or preparation of the manuscript.

**Competing Interests:** The authors have declared that no competing interests exist.

## Abstract

Neural crest cells (NCCs) are an embryonic migratory cell population with the ability to differentiate into a wide variety of cell types that contribute to the craniofacial skeleton, cornea, peripheral nervous system, and skin pigmentation. This ability suggests the promising role of NCCs as a source for cell-based therapy. Although several methods have been used to induce human NCCs (hNCCs) from human pluripotent stem cells (hPSCs), such as embryonic stem cells (ESCs) and induced pluripotent stem cells (iPSCs), further modifications are required to improve the robustness, efficacy, and simplicity of these methods. Chemically defined medium (CDM) was used as the basal medium in the induction and maintenance steps. By optimizing the culture conditions, the combination of the GSK3β inhibitor and TGFβ inhibitor with a minimum growth factor (insulin) very efficiently induced hNCCs (70–80%) from hPSCs. The induced hNCCs expressed cranial NCC-related genes and stably proliferated in CDM supplemented with EGF and FGF2 up to at least 10

passages without changes being observed in the major gene expression profiles. Differentiation properties were confirmed for peripheral neurons, glia, melanocytes, and corneal endothelial cells. In addition, cells with differentiation characteristics similar to multipotent mesenchymal stromal cells (MSCs) were induced from hNCCs using CDM specific for human MSCs. Our simple and robust induction protocol using small molecule compounds with defined media enabled the generation of hNCCs as an intermediate material producing terminally differentiated cells for cell-based innovative medicine.

## Introduction

In order to apply human pluripotent stem cells (hPSCs) to innovative medicine, such as cell therapy, disease modeling, and drug discovery, robust and efficient methods to produce the desired cell types without contaminating undesired cells are indispensable [1]. Since the contamination of hPSCs, in particular, may cause serious adverse effects, careful monitoring, which requires a considerable amount of time and cost, has to be conducted. Therefore, it would be beneficial to have intermediate cells between hPSCs and terminally differentiated cells, which are proved to have no contaminated hPSCs, contain limited but multiple differentiation properties, and stably proliferate without phenotypic changes. One of the promising candidates with such features is the neural crest cell (NCC) [2].

The neural crest emerges at the border of the neural and non-neural ectoderm in gastrula embryos during vertebrate development [3]. Cells in the neural crest, and later in the dorsal part of the neural tube, eventually delaminate and migrate throughout the body while retaining their characteristic phenotype [4]. When they reach their target tissues, NCCs differentiate into specific cell types depending on the location [5]. NCCs give rise to the majority of cranial bone, cartilage, smooth muscle, and pigmented cells in the cranial region, as well as neurons and glia in the peripheral nervous system [3–5]. Cardiac NCCs are known to contribute to valves in the heart, while vagal NCCs differentiate into enteric ganglia in the gut [6]. NCCs give rise to neurons and glia in the peripheral nervous system in the trunk region, secretory cells in the endocrine system, and pigmented cells in the skin.

Using a lineage-tracing system, rodent neural crest-derived cells were detected in adult tissues such as bone marrow, and still retained multipotent differentiation properties, which indicated that these cells are one of the cell-of-origin of multipotent mesenchymal stromal cells (MSCs) [7, 8]. Therefore, the production of human MSCs (hMSCs) from hPSCs via NCC lineage is a promising approach for the use of hPSCs in innovative medicine [9, 10]. A considerable number of studies have been dedicated to establishing robust and efficient induction methods from hPSCs to hNCCs in the past decade [11–13]. However, most of these studies used non-human stromal feeder cells or only achieved low induction

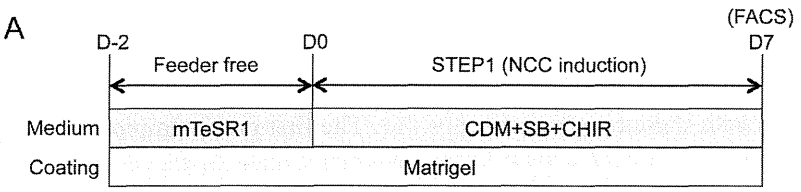


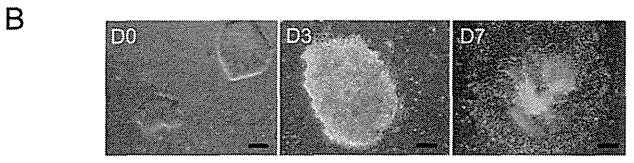


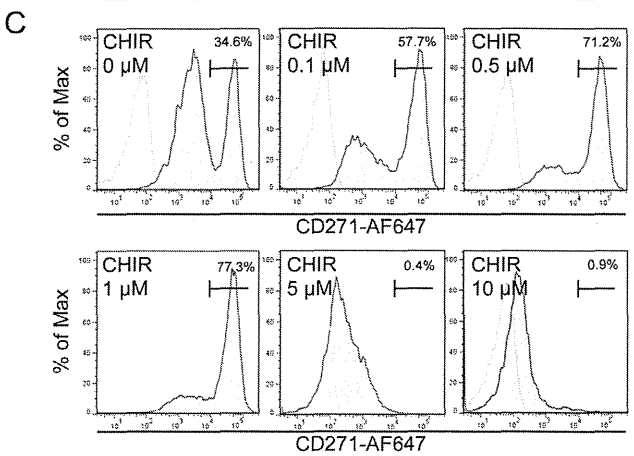


D

| Cell | Induction efficiency (%) |
|---|---|
| 414C2 | 73.5 ± 6.0 |
| 201B7 | 79.8 ± 2.6 |
| KhES1 | 75.7 ± 4.4 |
| KhES3 | 71.4 ± 4.8 |
| H9 | 75.0 ± 6.2 |

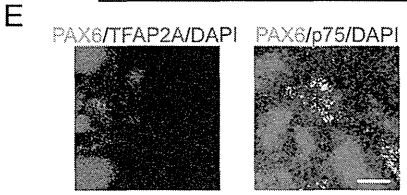


**Figure 1. Induction of p75$^{high}$ cells from hPSCs.** A) Schematic representation of the protocol. B) Morphology of colonies during the induction. Phase contrast images were taken on days 0, 3, and 7. Scale bar, 200 μm. C) The fraction of p75-positive cells in 201B7 cells was treated with SB431542 (SB) (10 μM) and CHIR99021 (CHIR) (indicated concentration) for seven days, stained with an anti-p75 antibody, and analyzed by FACS. D) Fraction of the p75$^{high}$ population induced by SB (10 μM) and CHIR (1 μM) from hESCs (KhES1, KhES3, H9) and hiPSCs (414C2, 201B7). Average ± SD. N=3, biological triplicate. E) Immunocytochemical analyses of colonies on day 7 (201B7). Cells were stained with antibodies against PAX6, TFAP2A, and p75. Scale bar, 100 μm.

doi:10.1371/journal.pone.0112291.g001